Pramāṇa – J. Phys., Vol. 33, No. 3, September 1989, pp. 365–379. © Printed in India.

Giant resonances in ^{90}Zr and ^{116}Sn

S KAILAS, A SAXENA**, P P SINGH*, Q CHEN*, D L FRIESEL*, P SCHWANDT* and E J STEPHENSON*

Nuclear Physics Laboratory, University of Washington, Seattle, Washington 98195, USA
*Indiana University Cyclotron Facility, Bloomington, Indiana 47405, USA
**Nuclear Physics Division, Bhabha Atomic Research Centre, Bombay 400085, India

MS received 9 January 1989

Abstract. The giant resonance region in ^{90}Zr and ^{116}Sn excited by 270 MeV helions has been measured up to about 35 MeV excitation energy. The low and the high energy octupole resonances are seen prominently in addition to the quadrupole and the monopole resonances. The angular distribution data for the various multipoles are satisfactorily explained by the collective model calculations. The percentatge energy weighted sum rule strengths have been determined for all the prominent resonances.

Keywords. Inelastic scattering; helium-3 particles at 270 MeV; zirconium-90; tin-116; giant resonances.

PACS Nos 24·30; 25·55

1. Introduction

In the past two decades or so, there have been a large number of investigations, both theoretical and experimental, whose motivation was to understand the giant resonance (GR) region of the nuclear excitation spectrum. The present status of the research in this field has been summarized by van der Woude (1987). Even though many experiments have been done using protons with energies up to 1 GeV, the ones using the complex ions have been mostly limited to energies < 50 MeV/nucleon. However, recently there have been a few experiments done utilizing higher energy alpha (Bonin *et al* 1984) and heavy ion beams (Bertrand *et al* 1988). Use of higher energy beams generally leads to larger cross sections for the various multipoles excited. Furthermore as the pick-up break-up bump shifts to higher excitation regions the GR region is free from this interference. It is expected (Morsch 1985) that the composition and the character of the continuum background will change as a function of the projectile type and the bombarding energy. Evidence for this has already come from high energy (p, p') experiments (Morsch 1985). It is anticipated (Bonin *et al* 1984) that use of higher energy light ions may offer a suitable experimental condition for observing a stronger GR signal above the background. In fact in the case of heavy ions like oxygen with $E/A = 85$ MeV, a strong enhancement of the GR over the background has been seen (Bertrand *et al* 1988).

We undertook an extensive study of the GR region excited in ^{58}Ni, ^{90}Zr, ^{116}Sn and ^{208}Pb targets using 270 MeV helions (90 MeV/nucleon) available from the Indiana University Cyclotron Facility (IUCF). The experiment was performed with the

motivation to confirm the presence of not only the already known GRs such as the giant quadrupole resonance (GQR) and the giant monopole resonance (GMR), but also to locate GRs with $L \geqslant 3$. The analysis and the results for the ^{58}Ni and ^{208}Pb targets have been reported elsewhere. (Kailas *et al* 1989). While the low energy octupole resonance (LEOR) and the high energy octupole resonance (HEOR) are rather weakly excited in ^{58}Ni and ^{208}Pb nuclei, they are fairly strongly excited in ^{90}Zr and ^{116}Sn nuclei, so that a careful analysis to extract their strengths has been made in the present work. In the following sections the experimental details, the results and the analysis for the ^{90}Zr and ^{116}Sn targets are presented.

2. Experimental details

Measurements of the differential cross section $\sigma(\theta)$ were carried out utilizing the 270 MeV helions, the highest energy available from IUCF. Isotopically enriched (>95%) targets of ^{90}Zr and ^{116}Sn of thickness 25·2 and 44·1 mgm/cm^2 respectively, were used for these measurements. The scattered helions were detected using a $\Delta E - E$ telescope consisting of intrinsic germanium detectors of 2 cm total thickness. The angular acceptance of the detectors was $\pm 0{\cdot}3°$. An overall energy resolution of better than 700 keV FWHM was obtained. The data were measured in the angular range $\theta = 8° - 20°$ for ^{90}Zr and $\theta = 8{\cdot}5° - 20^0$ for ^{116}Sn. In the present work, we have normalized the $\sigma(\theta)$ values obtained to earlier (Singh *et al* 1986) precise measurements made using the IUCF magnetic spectrometer. This normalization procedure led to an uncertainty of 5% in the $\sigma(\theta)$ values obtained here. The usual care was taken to minimize the beam dependent but target independent background in the GR region

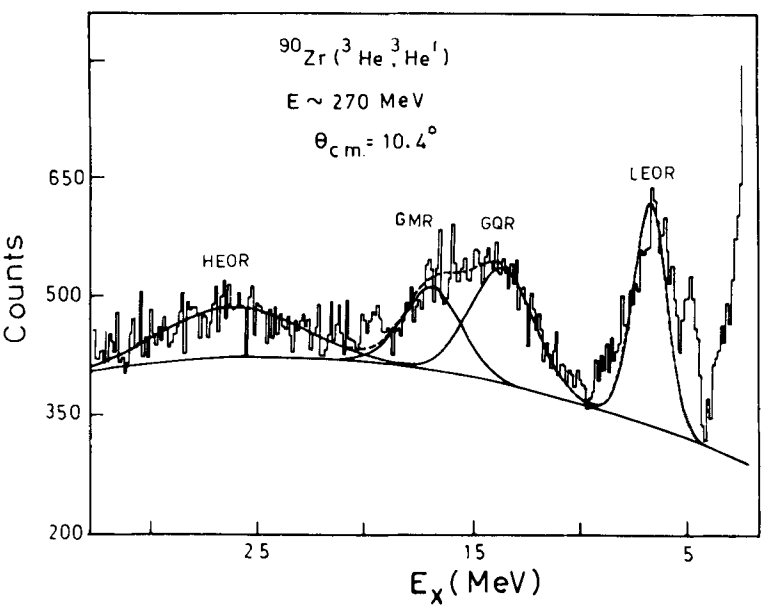

Figure 1. Energy spectrum for 270 MeV helions scattered from ^{90}Zr. The shapes of the assumed continuum background and the giant resonances are shown as continuous lines. The dashed line represents the sum of the various resonances which overlap.

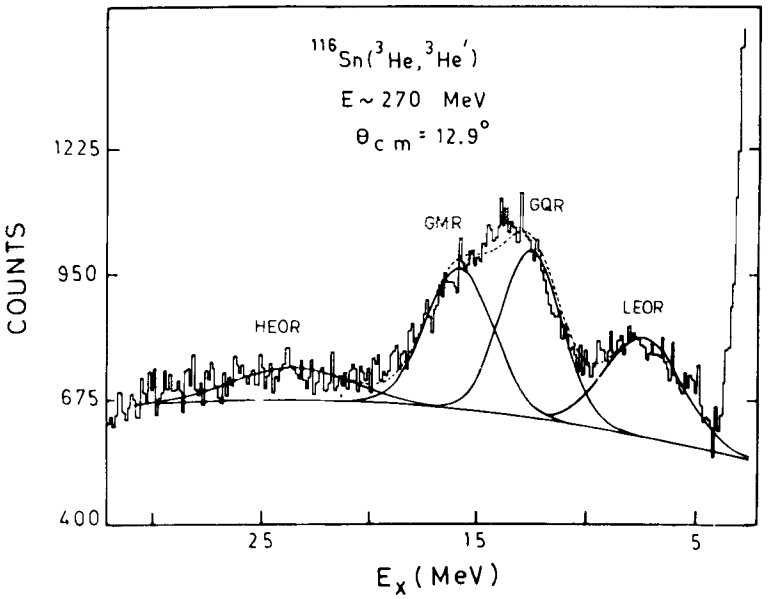

Figure 2. Energy spectrum for 270 MeV helions scattered from ^{116}Sn. The shapes of the assumed continuum background and the giant resonances are shown as continuous lines. The dashed line represents the sum of the various resonances which overlap.

of the spectra by periodically inserting an empty target frame with a smaller central hole and by proper tuning of the beam.

Typical energy spectra obtained for ^{90}Zr (at $\theta = 10{\cdot}4°$) and for ^{116}Sn (at $\theta = 12{\cdot}9°$) are shown in figures 1 and 2, respectively. The LEOR, the GQR, the GMR and the HEOR peaks appear rather prominently at the expected excitation energies. Detailed shape analysis of these spectra consisting of multipole peaks riding on a smooth background is reported in §3.

3. Analysis

3.1 *Experimental*

As a first step, a smooth background, usually a second order polynomial in excitation energy (van der Woude 1987; Kailas *et al* 1984) was drawn as shown in figures 1 and 2, to subtract out the assumed continuum background. It is well-known (van der Woude 1987) that the uncertainty involved in this procedure often leads to considerable error in the estimation of the multipole strength. However, this method of subtracting the background yielded satisfactory results mainly because the angular distribution of the background falls off almost exponentially with increasing θ, while that associated with any GR exhibits oscillations characteristic of the associated angular momentum (van der Woude 1987; Kailas *et al* 1989).

As pointed out before, there are three broad prominent structures corresponding respectively to the LEOR, the GQR, the GMR and the HEOR regions. We have analysed the whole excitation region consisting of four Gaussian peaks of the types mentioned above. The background was kept fixed throughout the analysis. At first

the widths and the centroids of the peaks were fixed at average values known from the other works (van der Woude 1987; Bonin *et al* 1984) and only the peak heights were varied to optimise the fits to the data. In the second stage the centroid positions were also varied to improve the quality of the fit. Finally the widths of the LEOR and the HEOR were suitably adjusted to obtain the overall best fit covering the whole excitation energy region. As can be seen from figures 1 and 2, the quality of the fits is satisfactory. The extracted angular distributions for the various regions are shown in figures 3 and 4 for ^{90}Zr and in figures 5 and 6 for ^{116}Sn targets respectively. The average widths Γ and the excitation energies E_x used in the present analysis are given in table 1.

3.2 *Theoretical*

Apriori knowledge of the angular distribution shapes for the various multipoles is very useful for judging how well one can separate the various L values which are expected to be present in the GR region of excitation. The angular distributions for the various L values were calculated using the computer code DWUCK-4 (Kunz 1982), starting with the optical model parameters determined (Singh *et al* 1986) from fits to the elastic data. Singh *et al* (1986) showed that this method of calculating the angular distribution shapes works well for the low-lying states. It is expected that we can extend these calculations with confidence to the GR region as well. The optical model parameters are listed in table 2.

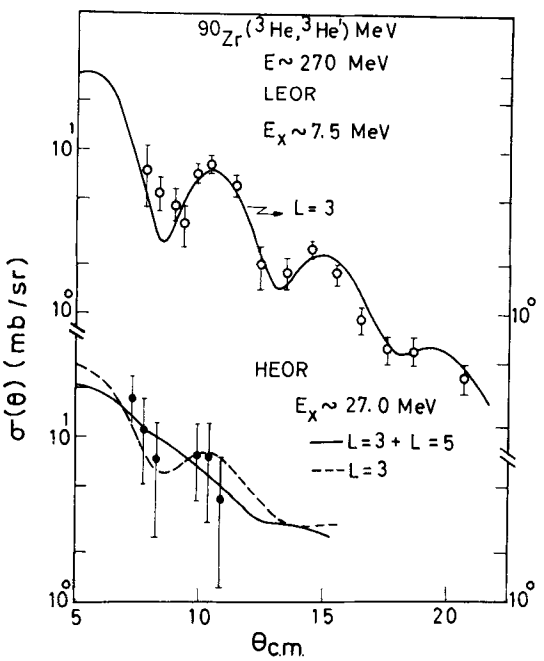

Figure 3. Angular distribution data for the LEOR and the HEOR in ^{90}Zr and theoretical fits obtained using the DWBA formalism. For the HEOR the fits obtained using a pure $L = 3$ and a mixture of $L = 3$ and $L = 5$ are shown.

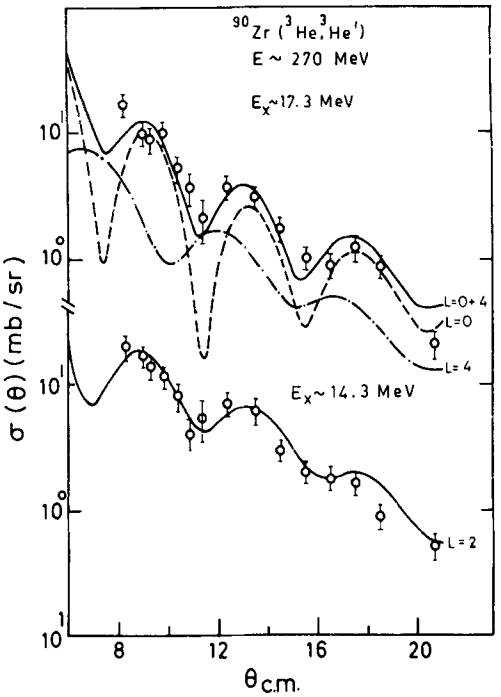

Figure 4. Angular distribution data for the GQR and the GMR regions in ^{90}Zr and theoretical fits obtained using the DWBA formalism. The contributions due to the various L values are shown separately.

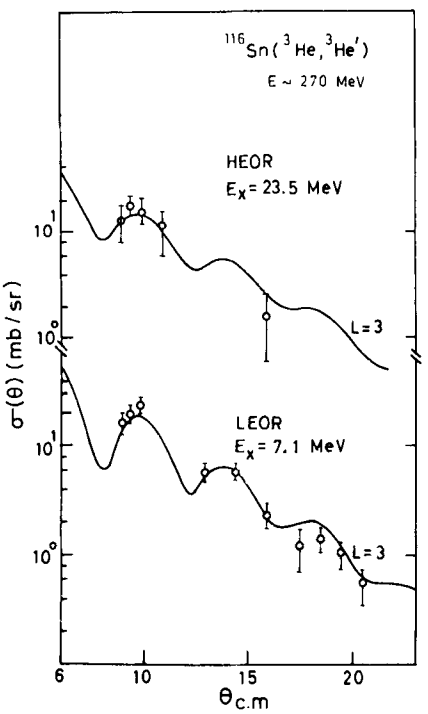

Figure 5. Angular distribution data for the LEOR and the HEOR in ^{116}Sn and theoretical fits obtained using the DWBA formalism.

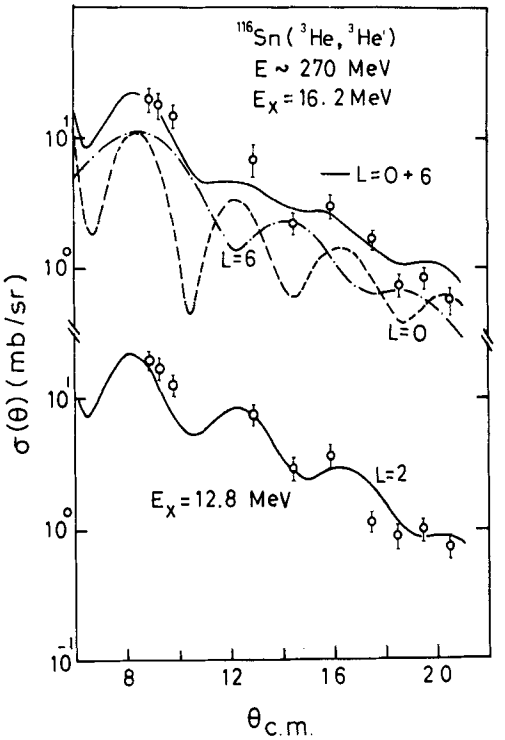

Figure 6. Angular distribution data for the GQR and the GMR regions in ^{116}Sn and theoretical fits obtained using the DWBA formalism. The contributions due to the various L values are shown separately.

Table 1. Parameters of the GR for the various E_x regions.

		^{90}Zr	^{116}Sn
LEOR	E_x (MeV)	7·5 ± 0·3	7·1 ± 1·9
	Γ (MeV)	1·9	4·2
GQR	E_x (MeV)	14·3 ± 0·4	12·8 ± 0·3
	Γ (MeV)	3·4	3·2
GMR	E_x (MeV)	17·3 ± 0·4	16·2 ± 0·4
	Γ (MeV)	3·1	3·6
HEOR	E_x (MeV)	27·0 ± 0·5	23·5 ± 0·6
	Γ (MeV)	7·0	6·0

For $L \geqslant 2$, the coupling form factor was taken as (Satchler 1983)

$$\beta_L A_T^{1/3}\left[r_R\left(\frac{dV}{dr}\right)_R + ir_I\left(\frac{dV}{dr}\right)_I\right]Y_{lm} \tag{1}$$

where the sufficies R and I respectively stand for the real and the imaginary parts of the optical potential. The form factor for the monopole was taken to be (version I

Table 2. 270 MeV optical model parameters.

	^{90}Zr	^{116}Sn
V_R (MeV)	69·0	66·0
r_R (fm)	1·24	1·27
a_R (fm)	0·83	0·86
V_I (MeV)	23·0	23·0
r_I (fm)	1·39	1·40
a_I (fm)	0·79	0·66

The potential is defined as

$$V(r) = V_C(r) - V_R f_R(r) - iV_I(r) f_I(r),$$

$$f_x(r) = \left[1 + \exp\left(\frac{r - r_x A_T^{1/3}}{a_x}\right)\right]^{-1}$$

$x = \mathrm{R}$ or I

and V_C = Coulomb potential with radius R_C

$$R_C = 1{\cdot}3 A_T^{1/3}$$

of Satchler (1983))

$$3(V_R f_R(r) + iV_I f_I(r)) + r\left(\frac{dV}{dr}\right)_R + ir\left(\frac{dV}{dr}\right)_I \tag{2}$$

where

$$f_x(r) = \left(1 + \exp\left(\frac{r - r_x A_T^{1/3}}{a_x}\right)\right)^{-1}$$

($x = \mathrm{R}$ and I stand for the real and the imaginary parts respectively).

The appropriate energy weighted sum rule strengths (EWSR) are given for $L \geqslant 2$ by (Satchler 1983)

$$S_L = \frac{\beta_m^2 R_m^2}{\frac{4\pi}{3A_T}\frac{\hbar^2}{2mE_x} L(2L+1)} \tag{3}$$

and for $L = 0$ by (Satchler 1983)

$$S_L = \frac{\beta_m^2 R_m^2}{\frac{4\pi}{3A_T}\frac{\hbar^2}{2mE_x} 5}. \tag{4}$$

Here the matter radius $R_m = 1{\cdot}2\ A_T^{1/3}$ and the associated deformation parameter β_m is defined as $\beta_m R_m = \beta_L R_{\mathrm{opt}}$ where $R_{\mathrm{opt}} = 0{\cdot}5\,(r_R + r_I)A_T^{1/3}$. The calculations reported in figures 7 and 8 were made assuming 100% EWSR strength. The Coulomb excitation contribution has been added for $L \geqslant 1$.

The angular distribution patterns calculated for $L = 0$ and $L = 2$ are very similar as far as positions of maxima and minima are concerned (see figures 7, 8). However, there are noticeable differences in their respective maxima to minima ratios. The $L = 4$ distribution is having maxima and minima positions shifted by about 1–1·5° with

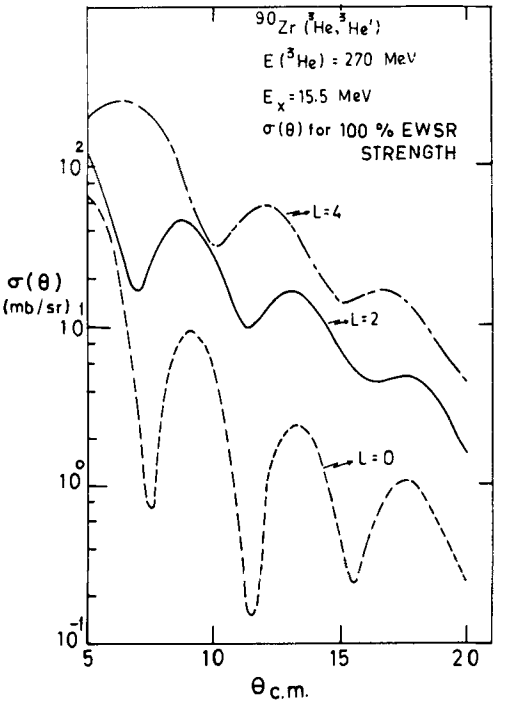

Figure 7. DWBA predictions for the inelastic scattering of helions from ^{90}Zr. The $L = 0$, 2 and 4 calculations are for 100% depletion of EWSR strength.

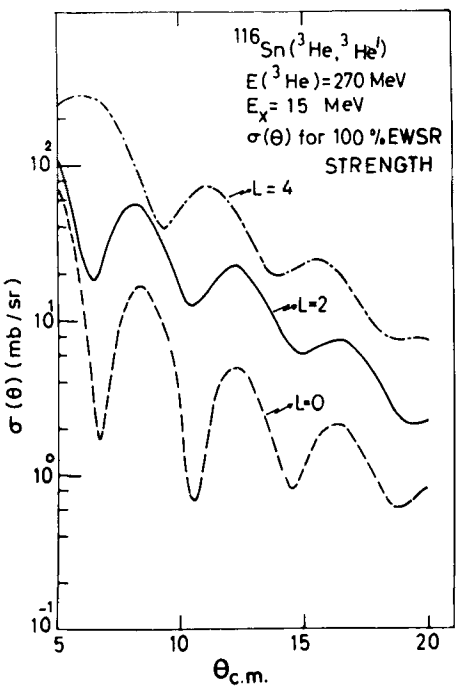

Figure 8. DWBA predictions for the inelastic scattering of helions from ^{116}Sn. The $L = 0$, 2 and 4 calculations are for 100% depletion of EWSR strength.

respect to the ones observed for $L = 2$. This feature offers the possibility of locating $L = 4$ strength in the presence of $L = 2$ strength.

4. Results

4.1 *Giant resonances in ^{90}Zr*

LEOR: The angular distribution for the structure around $E_x = 7{\cdot}5$ MeV, supposedly due to the LEOR is shown in figure 3. The continuous line is the DWBA calculation for $L = 3$ and it reproduces the data very well. The %EWSR strength for the LEOR has been determined to be $6 \pm 2\%$.

HEOR: The angular distribution for the broad structure around $E_x = 27$ MeV is given in figure 3. The number of data points is rather limited and the measurements also have large errors. Fitting the data assuming a pure $L = 3$ contribution led to a strength of $29 \pm 7\%$. However a combination of $L = 3$ (15%) and $L = 5$ (5%) yielded a marginally better fit to the data in terms of a chi-squared criterion.

GQR: The angular distribution for the GQR region ($E_x = 14{\cdot}3$ MeV), is very nicely reproduced by a pure $L = 2$ contribution (figure 4). The %EWSR strength is determined to be 38 ± 10. We have not tried to look for contributions from other L values in this region.

GMR: The angular distribution for the GMR region ($E_x = 17{\cdot}3$ MeV) is best fit assuming 112% $L = 0$ and 3% $L = 4$ contributions (figure 4). The importance of $L = 4$ contribution can be readily seen in the θ range 11° to 13°.

4.2 *Giant resonances in ^{116}Sn*

LEOR: The LEOR ($E_x = 6{\cdot}6$ MeV) angular distribution is well reproduced by a pure $L = 3$ contribution (figure 5). The resultant strength is $13 \pm 3\%$.

HEOR: The data for this region ($E_x = 23{\cdot}5$ MeV) is rather limited in angular range. A pure $L = 3$ calculation with $35 \pm 8\%$ strength explains the data (figure 5) fairly well.

GQR: The GQR region ($E_x = 12{\cdot}8$ MeV) is adequately explained by a pure $L = 2$ calculation (figure 6). For this resonance we have extracted a sum rule strength of 34%. We have not tried including $L = 4$ or $L = 6$ contributions in this region.

GMR: The GMR region ($E_x = 16{\cdot}2$ MeV) could not be fitted well by assuming a pure $L = 0$ contribution. Within the limited angular range covered in the present case there is an indication for the presence of $L = 6$ rather than $L = 4$, in particular for the data near $\theta = 14°$. We determine 72% strength for $L = 0$ and 5% strength for $L = 6$ (figure 6).

The results of the present analysis along with the other literature values are summarized in tables 3 to 7. To check the sensitivity of the %EWSR strengths on the assumed peak shapes, we have also analysed the GR data by integrating the cross section in the E_x region 10 to 20 MeV, (after subtracting the background) and fitting the resultant angular distributions with $L = 0$, 2 and 4(6) contributions. As $L = 0$ and $L = 2$ distributions are correlated, we varied the $L = 0$ strength in discrete steps and searched for the other multipoles $L = 2$ and $L = 4(6)$ to best fit the data. In the case of ^{90}Zr, varying the GMR strength from 25 to 75%, caused the GQR strength to change from 51 to 43%. The $L = 4$ strength more or less remained around 3·6%. Similarly, in making a change of GMR strength from 25 to 75% for ^{116}Sn, it was found that the GQR strength varied from 45 to 32% while the $L = 6$ strength remained

Table 3. Percentage energy weighted sum rule strengths for the giant monopole resonance (GMR) $L = 0$.

A. ^{90}Zr

E_x (MeV)	Γ (MeV)	%EWSR	Probe E(MeV)	Reference
17.3 ± 0.4	3·1	112 ± 40	^{3}He, 270	Present work
16.4 ± 0.3	3·6	29	^{3}He, 108·5	Buenerd (1984)
16.2 ± 0.5	3·5	90 ± 20	^{4}He, 129	Youngblood *et al* (1981)
17.5 ± 0.5	2·9	106 ± 26	^{4}He, 152	Bertrand *et al* (1980)
17.2 ± 0.5	4·3	20 ± 6	*d*, 108	Willis *et al* (1980)
17.5 ± 0.5	3	60 ± 25	*p*, 60	Bertrand *et al* (1979)
16·2	3·5	160 ± 20	π, 163	Ullmann *et al* (1987)

Average (%EWSR strength): 82 ± 18

B. $^{116}S_n$

16.2 ± 0.4	3·6	72 ± 30	^{3}He, 270	Present work
15.6 ± 0.3	3·2	34	^{3}He, 108·5	Buenerd (1984)
15.6 ± 0.3	4·1	180 ± 60	^{4}He, 129	Youngblood *et al* (1981)
15.8 ± 0.2	3	19 ± 7	^{4}He, 340	Bonin *et al* (1984)
16.0 ± 0.3	3·1	14 ± 7	^{4}He, 480	Bonin *et al* (1984)

Average (%EWSR strength): 64 ± 27

Table 4. Percentage energy weighted sum rule strengths for the giant quadrupole resonance (GQR) $L = 2$.

A. ^{90}Zr

E_x (MeV)	Γ (MeV)	%EWSR	Probe E(MeV)	Reference
14.3 ± 0.4	3·4	38 ± 10	^{3}He, 270	Present work
14.1 ± 0.3	4·0	37	^{3}He, 108·5	Buenerd (1984)
14.0 ± 0.2	3·4	66 ± 17	^{4}He, 129	Youngblood *et al* (1981)
14.1 ± 0.5	3·6	86 ± 17	^{4}He, 152	Bertrand *et al* (1980)
14.1 ± 0.5	4·3	40 ± 8	*d*, 108	Willis *et al* (1980)
14.2 ± 0.3	4·0	60 ± 15	*p*, 60	Bertrand *et al* (1979)
14·1		30 ± 8	*p*, 200	Bertrand *et al* (1981)
14·0	3·6	31 ± 3	π, 163	Ullmann *et al* (1987)
14·0		45	π, 226	Marty *et al* (1980)
		56 ± 17*	*e*, 150–250	Fukuda and Torizuka (1972)

Average (%EWSR strength): 48 ± 6
*Not included

B. ^{116}Sn

12.8 ± 0.3	3·2	34 ± 11	^{3}He, 270	Present work
13.2 ± 0.3	3·6	45	^{3}He, 108·5	Buenerd (1984)
13.2 ± 0.2	3·3	84 ± 25	^{4}He, 129	Youngblood *et al* (1981)
13.5 ± 0.2	4·0	$30 \pm {}^{8}_{6}$	^{4}He, 340	Bonin *et al* (1984)
13.5 ± 0.2	4·0	$32 \pm {}^{7}_{6}$	^{4}He, 480	Bonin *et al* (1984)
		120 ± 36*	*e*, 150–250	Torizuka *et al* (1975)

Average (%EWSR strength): 45 ± 9
*Not included

Table 5. Percentage energy weighted sum rule strengths for the low energy octupole resonance (LEOR) $L = 3$.

A. ^{90}Zr

E_x (MeV)	Γ (MeV)	%EWSR	Probe E(MeV)	Reference
7·5±0·3	1·9	6±2	^{3}He, 270	Present work
7·5±0·4	>2	19·5±2·8	^{3}He, 140	Yamagata *et al* (1981)
7·25±0·06	1·87	11·2	*p*, 65	Fujita *et al* (1985)
7·2±0·2	2·4	$22{\cdot}8\pm^{10}_{5}$	*p*, 800	DiGiacomo and Peterson (1979)
7·2	>2	20±5	^{4}He, 96	Moss *et al* (1978)
7·25	1·87	7±0·9	π, 163	Ullmann *et al* (1987)

Average (%EWSR strength): 14·4±2·6

B. ^{116}Sn

7·1±0·3	4·2	13±3	^{3}He, 270	Present work
7±0·4	>2·5	24	^{3}He, 110	Yamagata *et al* (1981)
6·5	>2·5	23±6	^{4}He, 115	Moss *et al* (1978)
7±0·5	1	8±5	^{4}He, 340	Bonin *et al* (1984)

Average (%EWSR strength): 17±4

Table 6. Percentage energy weighted sum rule strengths for the high energy octupole resonance (HEOR) $L = 3$.

A. ^{90}Zr

E_x (MeV)	Γ (MeV)	%EWSR	Probe E(MeV)	Reference
27·0±0·5	7	29±7	^{3}He, 270	Present work
26·5±1·5		47±20	^{3}He, 140	Yamagata *et al* (1981)
		18±4	p, 200	Bertrand *et al* (1981)

Average (%EWSR strength): 31±7

B. ^{116}Sn

23·5±0·6	6	35±8	^{3}He, 270	Present work
24·4±1·5		65±14	^{3}He, 140	Yamagata *et al* (1981)
22·9±1·0	6·5	22±6	*p*, 800	Carey *et al* (1980)
23·5±0·3	5·0	10±4	^{4}He, 340	Bonin *et al* (1984)
23·2±0·3	4·5	8±3	^{4}He, 480	Bonin *et al* (1984)

Average (%EWSR strength): 28±9

Table 7. Percentage energy weighted sum rule strengths for GR of $L = 4$ multipolarity.

Nucleus	E_x (MeV)	%EWSR	Probe E(MeV)	Reference
^{90}Zr	10–20	$3{\cdot}3 \pm 1{\cdot}1$	^{3}He, 270	Present work
	14·1	5	p, 200	Bertrand *et al* (1981)
		5–10	α, 104	Fuchs *et al* (1985)
Average (%EWSR strength): $5{\cdot}3 \pm 0{\cdot}9$				
^{116}Sn	10–20	<1	^{3}He, 270	Present work
	12·5	8 ± 4	^{4}He, 340	Bonin *et al* (1984)
	12	9 ± 3	^{4}He, 480	Bonin *et al* (1984)
Average (%EWSR strength): 6 ± 2				

around 4·3%. It appears from this analysis that the GQR and the higher L strengths obtained by the two types of analyses are consistent with each other and hence are not strongly dependent on the peak shapes assumed.

5. Discussion

Before making the actual comparison of our results with the ones from the literature, we have normalised the latter ones suitably to take care of the differences in the formulae or procedure used in extracting the %EWSR strengths. Willis *et al* (1980) and Buenerd *et al* (1979) use the imaginary potential radius to determine the sum rule strenghts. In our method, we take the average of the real and the imaginary potential radii and use it to get the %EWSR strengths. In view of this the strenghts quoted by the above two works have been normalized downwards by approximately 25%. Bertrand *et al* (1980) do not seem to be converting the β_L obtained from DWBA analysis to β_m before determining the strengths. To take care of this we have normalised their values upwards by about 30%. Bonin *et al* (1984) use the formula

$$\beta_L(A_p^{1/3} + A_T^{1/3}) = \beta_L^B A_T^{1/3}$$

(β_L^B denotes β_L of Bonin's work) to obtain β_L^B to be used in the %EWSR calculation. Normally one uses the form $\beta_L\, R_{\text{opt}} = \beta_L^P\, R_m$ (β_L^P denotes the new value of Bonin *et al* as used in the present work) where $R_{\text{opt}} = (R_R + R_I)/2$ and $R_m = 1{\cdot}2\, A_T^{1/3}$ (R_R and R_I are the real and the imaginary potential radii respectively). From the above relations we get the renormalisation factor $N = (\beta_L^P/\beta_L^B)^2$. In the case of ^{116}Sn the value of N works out to be 0·688 at 340 MeV and 0·654 at 480 MeV. The %EWSR strengths obtained by Bonin *et al* (1984) have been normalised by these factors. We have applied the normalisation only in those cases where the authors have given explicitly the various relevant details involved in the calculation.

GMR: While going through the GMR strengths listed in table 3, we see that the GMR strength for ^{90}Zr deduced here is (within errors) in accord with most other literature values (exceptions are Willis *et al* 1980 and Buenerd 1984). The one obtained here for ^{116}Sn lies within the large range of values available from the literature (table 3). A large discrepancy is noted between the results obtained by Bonin *et al* (1984)

and Youngblood *et al* (1981). While the value obtained by Bonin *et al* (1984) is unusually small, the one determined by Youngblood *et al* (1981) is abnormally large $>100\%$. This difference can be partly understood in terms of the differences in the Γ used in the two works. However, in ^{90}Zr the value obtained by Willis *et al* (1980) is the lowest inspite of their choice of the largest value of Γ.

GQR: In ^{90}Zr there exists a large number of works to compare with the present work. The %EWSR strength obtained in the present work, $38 \pm 10\%$, is consistent with the literature values which vary between 30 and 65% (except Bertrand *et al* 1980). An average value for all the determinations (except the electron scattering data of Fukuda and Torizuka (1972)) is $48 \pm 6\%$ which is in good agreement with the present work. In ^{116}Sn our result is in agreement with those of Bonin *et al* (1984) obtained using 340 and 480 MeV alpha particles and Buenerd (1984) obtained using 108·5 MeV helions. Youngblood *et al* (1981) obtained a value of 84% which is a factor of two higher than the present value. It is worth noting that Bonin *et al* (1984) get a lower value inspite of using a fairly large value of Γ. The results are summarized in table 4.

LEOR: The LEOR values obtained for ^{90}Zr can be grouped into two categories; one set lies close to 10% and the other is nearer to 20%. As we have analysed only a single prominent structure in the LEOR region (figure 3) it is possible that our value is low. In ^{116}Sn it is found that the results of higher-energy ^{3}He(present) and ^{4}He(Bonin *et al* 1984) measurements agree with each other. The lower-energy measurements (Yamagata *et al* 1981; Moss *et al* 1978) determine values which are almost twice as large as their higher-energy counterparts.

HEOR: Within errors the HEOR strength obtained in the present work for ^{90}Zr is consistent with values from the literature, which vary between 18 and 47%. For ^{116}Sn our value lies within the large range of values obtained by others. While the ones determined by Bonin *et al* (1984) is on the lower side, the ones obtained by Yamagata *et al* (1981) is on the higher side. The results are summarized in table 6.

$L = 4$ strength: The $L = 4$ strength determined for ^{90}Zr is in agreement with the value obtained by Bertrand *et al* (1981) using 200 MeV protons. This result is consistent with the strength of 5 to 10%, in the E_x range of 13 to 16 MeV, determined from the neutron decay of GR in ^{90}Zr excited through the inelastic scattering of 104 MeV alpha particles (Fuchs *et al* 1985). While we have observed negligible $L = 4$ strength in ^{116}Sn but a few per cent $L = 6$ strength, Bonin *et al* (1984) obtained 4 to 12% $L = 4$ strength.

Referring tables 3–7, we do find differences in many cases in the E_x and Γ values used by different groups. In addition, there are also differences the way the background continuum contributions are estimated. The variations in the %EWSR strengths are mainly due to these differences mentioned above. Serr *et al* (1983) have already pointed out that considerable differences (20 to 50%) in the %EWSR strengths may result from the above mentioned reasons. We felt that it may be worthwhile to determine the average of all the literature values (unweighted) for each of these resonances which may then be used for comparison with the theoretical predictions. These average values are given in tables 3–7. The electron scattering results have not been included in obtaining these averages. Comparison of the individual results with the average values may throw some light on the probe dependence of the βR values (%EWSR strengths) determined using different projectiles (Bernstein *et al* 1983). The theoretical values of Krewald and Speth (1974) are in general very high as compared to the experimental values obtained for ^{90}Zr. They do not have predictions for ^{116}Sn. For

^{120}Sn Soloviev *et al* (1977) get a value 30% for the GQR which compares favourably with the average value of $45 \pm 9\%$ obtained here. For the octupole resonances, one can compare the present results with the theoretical predictions of Bortignon and Broglia (1981). For ^{90}Zr, they predict, %EWSR strengths of 14 and 39 respectively for the LEOR and for the HEOR, which are in good agreement with the corresponding average experimental values of $14 \pm 3\%$ and $31 \pm 7\%$ respectively. Similarly for ^{120}Sn their values are 11% and 30% which are consistent with the respective experimental values of $17 \pm 4\%$ and $28 \pm 9\%$ obtained for ^{116}Sn. For ^{90}Zr, Serr *et al* (1983) get 76% strength for the GQR with a Γ of 4 MeV. This is on the high side of the average value of $48 \pm 6\%$. They also get 92% strength for the monopole and 39% strength for the HEOR, consistent with the average experimental values. Generally the widths predicted by the theoretical calculations are in fair agreement with the experimental determinations.

6. Conclusion

We have been able to identify reliably the LEOR, the GQR, the GMR and the HEOR regions in ^{90}Zr and ^{116}Sn and obtain the %EWSR strengths for these resonances. The extracted GQR strengths are in good agreement with the average values from the literature. The octupole strengths are found to be of the right order when comapred to the other experimental or theoretical values. We do find a few per cent $L = 4$ strength in ^{90}Zr and $L = 6$ strength in ^{116}Sn, in the GMR region. Within the uncertainties involved in the various analysis procedures (the subtraction of the background continuum and the extraction of the %EWSR strengths) it appears that only $\approx 50\%$ of the $L = 2$ strength is seen in the GQR region. However, there is still considerable strength either buried in the continuum background or spread out to higher excitation energy regions. In using 90 MeV/nucleon helion beam we have not gained substantially in the observed ratio of the GR signal (GQR + GMR region) to the background as compared to that obtained using lower energy helions. There is a significant improvement however in the HEOR signal observed in the present work over that obtained using lower energy helions. It appears that even after employing higher energy complex ions around 100 MeV/nucleon, we have not been able to locate the presence of concentrated strengths for higher order multipoles ($L \geqslant 4$) in the excitation region up to 40 MeV. This is in agreement with the expectation that these strengths are broadly spread out in energy. A better knowledge of the continuum is essential in estimating its contribution in a more definite way, thereby facilitating more reliable determination of the %EWSR strengths for not only $L \leqslant 2$ resonances but also higher-order multipole resonances.

Acknowledgements

Prof. M L Sehgal was an active member of this programme until his untimely death. The authors thank Prof. K A Snover for a critical reading of the manuscript and the useful comments. This work was supported in part by the National Science Foundation, USA and the Departments of Energy, USA and India.

References

Bernstein A M, Brown V R and Madsen V A 1983 *Comments Nucl. Part. Phys.* **11** 203

Bertrand F E, Satchler G R, Horen D J and van der Woude A 1979 *Phys. Lett.* **B80** 198

Bertrand F E, Satchler G R, Horen D J, Wu J R, Bacher A D, Emery G T, Jones W P, Miller D W and van der Woude A 1980 *Phys. Rev.* **C22** 1832

Bertrand F E, Gross E E, Horen D J, Wu J R, Tinsley J, McDaniels D K, Swanson L W and Liljestrand R 1981 *Phys. Lett.* **B103** 326

Bertrand F E, Beene J R and Horen D J 1988 *Proc. first topical meeting on giant resonance excitation in heavy ion collisions*, Legnaro, 1987 (ed) P F Bortignon, J J Gaardhoje and M Di Toro, 1988 *Nucl. Phys.* **A482** 287c

Bonin B, Alamanos N, Berthier R, Bruge G, Faraggi H, Legrand D, Lugol J C, Mittig W, Papineau L, Yavin A I, Scott D K, Levine M, Arvieux J, Farvacque L and Buenerd M 1984 *Nucl. Phys.* **A430** 349

Bortignon P F and Broglia R A 1981 *Phys. Lett.* **B102** 303

Buenerd M, Bonhome C, Lebrun D, Martin P, Chauvin J, Duhamel G, Perrin G and de Saintignon P 1979 *Phys. Lett.* **B84** 305

Buenerd M 1984 *J. Phys.* **45** C4-115

Carey T A, Cornelius W D, DiGiacomo N J, Moss J M, Adams G S, McClelland J B, Pauletta G, Whitten C, Gazzaly M, Hintz N and Glashausser C 1980 *Phys. Rev. Lett.* **45** 239

DiGiacomo N J and Peterson R J 1979 *Phys. Rev.* **C20** 693

Fuchs K, Eyrich W, Hofmann A, Muhldorfer B, Scheib U, Schlosser H and Rebel H 1985 *Phys. Rev.* **C32** 418

Fujita Y, Fujiwara M, Morinobu S, Katayama I, Yamazaki T, Itahashi T, Ikegami H and Hayakawa S I 1985 *Phys. Rev.* **C32** 425

Fukuda S and Torizuka Y 1972 *Phys. Rev. Lett.* **29** 1109

Kailas S, Singh P P, Friesel D L, Foster C C, Schwandt P and Wiggins J 1984 *Phys. Rev.* **C29** 2075

Kailas S, Saxena A, Singh P P, Chen Q, Schwandt P and Stephenson E J 1989 *Nucl. Phys. A* (in press)

Krewald S and Speth J 1974 *Phys. Lett.* **B52** 295

Kunz P D 1982 DWUCK-4, University of Colorado version 1982 (unpublished)

Marty N, Morlet M, Willis A, Perrin C, Beveridge J L, Egger J P, Goetz F, Gretillat P, Johnson R R, Lunke C and Schwarz E 1980 *Z. Phys.* **A298** 149

Morsch H P 1985 *Proc. Niels Bohr Centennial Conf., Copenhagen, Nuclear Structure* (ed) R Broglia, G Hagemann and B Herskind, p. 433

Moss J M, Brown D R, Youngblood D H, Rosza C M and Bronson J D 1978 *Phys. Rev.* **C18** 741

Satchler G R 1983 *Direct nuclear reactions* (Oxford: Oxford University press)

Serr F E, Bortignon P F and Broglia R A 1983 *Nucl. Phys.* **A393** 109

Singh P P, Li Q, Schwandt P, Jacobs W W, Saber M, Stephenson E J, Saxena A and Kailas S 1986 *Pramāṇa – J. Phys.* **27** 747

Soloviev V G, Stoyanov Ch and Vdovin A I 1977 *Nucl. Phys.* **A288** 376

Torizuka Y, Kojima Y, Saito T, Itoh K and Nakada A 1975 *Res. Rep. Lab. Nucl. Sci. Tohoku Univ.* **6** 165

van der Woude A 1987 *Prog. Nuclear and Particle Physics* 18 217 (ed) A Faessler (Oxford: Pergamon press)

Willis A, Marty N, Frascaria R, Djalali C and Comparat V 1980 *Nucl. Phys.* **A344** 137

Yamagata T, Kishimoto S, Yuasa K, Iwamoto K, Saeki B, Tanaka M, Fukuda T, Miura I, Inoue M and Ogata H 1981 *Phys. Rev.* **C23** 937

Youngblood D H, Bogucki P, Bronson J D, Garg U, Lui Y W and Rozsa C M 1981 *Phys. Rev.* **C23** 1997